Effect of pretreated cow dung fiber on rheological and fatigue properties of asphalt binder

Niu, Dongyu; Zhang, Zhao; Gao, Yangming; Li, Yuanxiao; Yang, Zhengxian; Niu, Yanhui

DOI
10.1007/s10570-023-05113-y

Publication date
2023

Document Version
Final published version

Published in
Cellulose

Citation (APA)
Niu, D., Zhang, Z., Gao, Y., Li, Y., Yang, Z., & Niu, Y. (2023). Effect of pretreated cow dung fiber on rheological and fatigue properties of asphalt binder. *Cellulose*, *30*(6), 3773–3791. https://doi.org/10.1007/s10570-023-05113-y

Cellulose (2023) 30:3773–3791
https://doi.org/10.1007/s10570-023-05113-y

ORIGINAL RESEARCH

Effect of pretreated cow dung fiber on rheological and fatigue properties of asphalt binder

Dongyu Niu · Zhao Zhang · Yangming Gao · Yuanxiao Li · Zhengxian Yang · Yanhui Niu

Received: 8 October 2022 / Accepted: 22 February 2023 / Published online: 10 March 2023

Abstract Cow dung waste has caused severe environmental pollution and public health issues in China. In this study, the cow dung residues were used as a cheap renewable fiber to modify asphalt binder, providing a new solution for the proper disposal of cow dung waste. Three cow dung fibers with two lengths were prepared using different treatments, including original cow dung fiber (CDF), surface treatments of cow dung fiber (STCDF) and alkali treatments of cow dung fiber (ATCDF). The physicochemical properties of CDF, STCDF and ATCDF were analyzed by scanning electron microscope (SEM) and thermogravimetry (TG). The viscidity, rheological properties and fatigue characteristics of CDF modified asphalt binders (CDFMA) were evaluated using Brookfield viscometer and dynamic shear rheometer. The results showed that the rough surfaces of STCDF and ATCDF improved their thermal stability. STCDF and ATCDF enhanced the resistance to permanent deformation under high temperature conditions of modified asphalt binder. STCDF modified asphalt binders exhibited the best viscosity and rheological performance. The increase of fiber length was positively correlated with the high temperature deformation resistance of CDFMA. CDF, STCDF and ATCDF inhibited fatigue cracking of modified asphalt binders compared to base asphalt binders. ATCDF modified asphalt binders exhibited higher fatigue life and

D. Niu · Z. Zhang · Y. Niu
Engineering Research Center of Transportation Materials of the Ministry of Education, Chang'an University, Xi'an 710061, Shaanxi, China

D. Niu · Z. Zhang · Y. Niu
School of Materials Science and Engineering, Chang'an University, Xi'an 710061, China

Y. Gao (✉)
Faculty of Civil Engineering and Geosciences, Delft University of Technology, Stevinweg 1, 2628 CN Delft, The Netherlands
e-mail: Y.Gao-3@tudelft.nl

Y. Gao
School of Civil Engineering and Built Environment, Liverpool John Moores University, Byrom Street, Liverpool L3 3AF, UK

Y. Li
College of Animal Science and Technology, Henan University of Science and Technology, Luoyang 471003, Henan, China

Z. Yang
Fujian Provincial University Research Center for Advanced Civil Engineering Materials, Fuzhou University, Fuzhou 350116, China

Z. Yang
College of Civil Engineering, Fuzhou University, Fuzhou 350116, Fujian, China

smaller crack under the same cyclic loading. The increase in fiber length had a slight improvement on the fatigue resistance of modified asphalt binders.

Keywords Cow dung fiber · Modified asphalt binder · Surface treatment · Rheological properties · Fatigue cracking

Introduction

Dairy industry is considered to be one of the fastest growing industries in the world. The current global dairy market has an estimated value of 673.8 billion dollars, which is expected to exceed one trillion dollars by 2024 (Iwuozor et al. 2022). It has been reported that the number of cattle in the world reached 987.51 million in 2020 (Ananno et al. 2021). Global demand for cow is still growing continually. The situation is the same in China. It is estimated that there are approximately 12.7 million cows in China, producing 260 million kilograms of cow dung per day (Rath et al. 2016). As a result, increasing amount of cow dung is produced and causes environmental pollution and public health issues due to the releases of toxic gases, odors and harmful bacteria (Masud et al. 2019).

Cow dung is an undigested plant material from the ruminant digestive system of cow, which includes reticulum, rumen, omasum and abomasum chambers. Raw food materials are swallowed by cow into the rumen and reticulum without adequate chewing. The semi-digested materials are moved from the two chambers back to the oral cavity. Then the ruminant materials are re-chewed and re-swallowed, and excreted from the body as residues passing through the omasum and abomasum (Gupta et al. 2016), as shown in Fig. 1. Cow dung contains a 3:1 ratio of urine to feces and the main components are lignin, cellulose and hemicellulose (Thangavel and Gopal 2017). Owing to the lack of effective treatment, the accumulation of a substantial amount of cow dung causes serious pollution as well as occupies the limited production area of the dairy farm. Therefore, the comprehensive utilization of cow dung into a worthwhile value-added product for human beings has become an urgent issue. In this regard, extensive studies have been attempted and cow dung has been used for biofertilizer production (Bridget et al. 2020; Hendarto et al. 2019) as a reinforcing phase material for friction composites (Manikandan et al. 2020; Yunhai et al. 2019), a source of solid fuel and energy (Marin-Batista et al. 2020; Narayan et al. 2018; Szymajda and Joka 2021), and a sorbent with great potential for the removal of wastewater pollutants and heavy metals (Dongjin et al. 2018; Ojedokun and Bello 2016). However, it is still very challenging to recycle and reuse cow dung on a large scale at present due to financial limitations and the technical deficiencies of solid waste management.

Considering the abundance of cellulose in cow dung, it can be used as natural fiber in road materials after recycling, which provides a promising solution to the accumulation of cow dung. Recent studies have shown that the cow dung fibers can be applied to cementitious materials and can effectively inhibit the development of self-shrinkage of the cementitious paste (Li et al. 2022). In terms of asphalt-based materials, recent research focuses on turning waste into cleaner asphalt pavement materials (Hl et al.

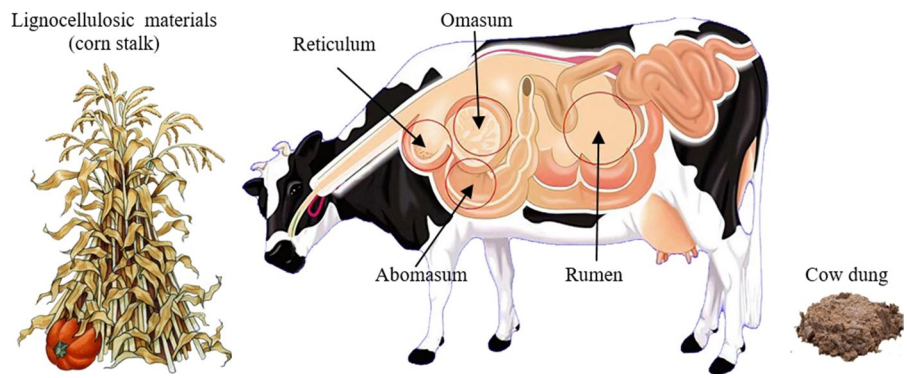

Fig. 1 The conversion of lignocellulose into cow dung

2022). Among them, natural fibers have been proven to be used as modifiers to improve the properties of asphalt pavement because of renewability and low cost. For instance, bamboo fibers incorporated into dense-grade and stone matrix asphalt (SMA) concrete can enhance dynamic stability and low-temperature crack resistance (Sheng et al. 2019); Corn straw fibers compounded with asphalt can effectively reduce the temperature sensitivity and increase the stiffness of the binder (Chen et al. 2019); Md Tareq Rahman et al. confirmed the rationality of the application for cigarette fiber modified asphalt (Rahman et al. 2020). These studies provide the basis for the effective role of biomass fibers in modified asphalt. However, the inertia and incompatibility of fiber with asphalt make it difficult to prepare fiber modified asphalt, limiting the application of the composite material (Su et al. 2019). To promote the wettability of the asphalt matrix to the natural fibers and enhance the interfacial adhesion of the composite, current researches mostly focus on the surface treatment of fibers before the preparation of modified asphalt, including alkali treatment (Adeyi et al. 2021; Chen et al. 2021), interfacial coupling treatment (Huda et al. 2008; Xiang et al. 2018), steam blasting treatment (Brugnago et al. 2011), heat treatment (Min et al. 2001), etc. Among them, alkali treatment and interfacial coupling treatment are commonly employed owing to the convenience of operation and good treatment effect. Despite numerous studies have been conducted on the surface treatment methods of plant fibers, few studies focus on comparing the effects of different treatment methods on fibers. In addition, numerous studies have shown that the rheological properties of asphalt binders can be more appropriately characterized employing master curves and black diagrams (Wang et al. 2019, 2020). However, few studies have comprehensively evaluated the rheological properties of fiber-modified asphalt binders from this aspect.

On the other hand, the effect of natural fibers on the fatigue failure of asphalt matrix is worthy of attention. Existing studies mostly adopt fatigue factor ($|G^*| \cdot \sin \delta$), dissipative energy ratio (DER) and dissipative energy change rate (RDEC) to evaluate the fatigue performance of modified asphalt binder, which has been proved that these parameters are incapable of correlating to the fatigue life of pavement (Zhou et al. 2013), and the fatigue mechanism are still unclear (Gao et al. 2020a). In addition, linear sweep test (LAS) test has gradually become an effective method to predict and evaluate the fatigue performance of asphalt binder based on the viscoelastic continuum damage (VECD) mechanics (Hintz and Bahia 2013a, b; Safaei and Castorena 2017). Nevertheless, the excessive strain amplitude of LAS test may lead to premature cracking of the asphalt binder and cannot explain how fatigue cracks evolve under rotational shear loading. To intuitively understand the fatigue damage mechanism of asphalt, several studies have focused on crack propagation in asphalt. For example, Hintz and Bahia used time sweep (TS) testing and digital visualization of DSR to observe crack growth trends in asphalt samples (Cassie Hintz and Bahia 2013a, b); Shan, Tian et al. used experimental and image analysis methods to determine the internal crack growth of asphalt samples during shear fatigue crack expansion (Shan et al. 2016). It was found that the fatigue cracking of asphalt specimens under rotational shear fatigue loading was "edge crack". Based on damage mechanics, Zhang and Gao developed a DSR-based cracking (DSR-C) model to accurately predict fatigue cracking in asphalt samples, which can be obtained by material properties in undamaged and damaged conditions (Zhang and Gao 2019). The DSR-C model has been widely used to characterize the fatigue resistance of various asphalt binders (Elo et al. 2020; Li et al. 2021; Yga et al. 2021).

The objective of this study is to investigate the rheological and fatigue characteristics of cow dung fiber modified asphalt binders with the effects of surface treatment and fiber length. Six kinds of cow dung fiber modified asphalt binders were prepared by using cow dung fibers as modifiers after surface and length treatments. Microscopic morphology and thermal stability of original fiber and two types of pretreated cow dung fibers were measured by scanning electron microscope (SEM) and thermogravimetry (TG). The rotational viscosity test, frequency sweep test, multiple stress creep recovery (MSCR) test, linear amplitude sweep (LAS) test and the time sweep test were conducted to evaluate the viscidity, rheological properties and fatigue characteristics of various modified asphalt binders.

Materials and methods

Raw materials

Base asphalt binder

In this research, AH-70 asphalt (PG 64–28) was selected as the base asphalt. Table 1 shows the measured basic properties of the asphalt binder and the relevant tests were carried out in accordance with Chinese Standards (JTG E20-2011). The AH-70 asphalt has also been measured following SHRP specifications and determined to be a PG 64–28 binder.

Cow dung fiber

The cow dung fibers used in this study were undigested plant fibers recovered from the excreta of cows that have been preliminarily dried and drained, which were obtained from Luoyang Zhuoer Animal Husbandry Co. LTD. The appearance of the dried and standing cow dung fibers was yellow, and the surface was not damaged or moldy. However, the loose structure and weak strength of cow dung fibers result in a poor compatibility with asphalt binder, which is difficult to form a stable structure. Therefore, the surface of cow dung fibers must be further pretreated before it is used in asphalt.

Table 1 Basic properties of AH-70 asphalt

Properties	Value	Requirement	Test method
Penetration (25 ℃, 0.1 mm)	67	60 ~ 80	T0604-2011
Penetration index (PI)	−0.5	−1.5 ~ +1.0	T0604-2011
Softening point (℃)	48.0	≥ 45	T0606-2011
Ductility (15 ℃)	> 100	≥ 100	T0605-2011
Wax content (%)	1.6	≤ 2.2	T0615-2011
Flash point (℃)	310	≥ 260	T0611-2011
Dynamic viscosity (60 ℃)	200	≥ 160	T0620-2000
Density (15 ℃, g/cm^3)	1.045	–	T0603-2011

Firstly, the cow dung fibers were sieved by a set of grids, and the residual fibers on the 0.6 mm sieve were selected as the original cow dung fibers (CDF). In addition, according the results of the different fiber length effects on the asphalt performance (Xing et al. 2020), two different lengths were produced (1 mm and 2 mm) to investigate the effect of cow dung fiber length on the properties of asphalt binder, as shown in Fig. 2.

Secondly, for the elimination of reactive hydroxyl groups (−OH) present in the extracted fibers, two common chemical treatments (alkaline treatment and silane treatment) were used on CDF with two lengths. This will diminish the water sensitivity of CDF and effectively interlock the matrix asphalt and CDF by increasing the surface roughness of the fibers (Aravinth et al. 2022):

(1) Absolute ethanol and distilled water were prepared in the ratio of 3:7. Then, 2% (by mass of ethanol) KH-570 (silane coupling agent) was added to the above solution. The mixture was thoroughly stirred and allowed to stand for 30 min to fully hydrolyze the silane coupling agent. After that, the CDF were added to the solution prepared above and soaked for 60 min. Finally, the CDF were filtered out and dried in an 80 ℃ oven for 3 h. The samples obtained in this step

Fig. 2 External appearance of CDF (1 mm and 2 mm)

were labelled as the surface treatments of cow dung fiber (STCDF).

(2) Another group of CDF was pretreated by alkali immersion and surface activity treatment: the fiber was soaked in sodium hydroxide solution with a concentration of 1 mol/L for 1 h at first, and then the surface pretreatment was carried out according to the step (1). This group was labelled as the alkali treatments of cow dung fiber (ATCDF).

Preparation of cow dung fiber modified asphalt (CDFMA).

Because the integrity of fibers may be destroyed by using high-speed shearing equipment to produce the fiber modified asphalt binder, which will diminish the modification effectiveness. Therefore, the method of low-speed continuous shearing was adopted in this study to prepare the CDFMA, and the specific process is as follows:

The AH-70 asphalt was first preheated to 160 ℃. The above-mentioned weighed (1.5 wt.%) cow dung fibers were then gradually added to the asphalt. After raising the temperature to 165 ℃, the fibers were completely dispersed in asphalt by low-speed shearing for 450 min at 165 ℃ at a speed of 2000 r/min.

Table 2 shows the identifications of the asphalt binders modified by the cow dung fibers used in this paper. Where BA represents the binder obtained from AH-70 asphalt after shearing at 165 °C for 45 min, which is to eliminate the potential effects of asphalt aging.

Experimental methods

Scanning electron microscope (SEM) analysis

The surface texture is an important index to study the influence of different pretreatment methods on the properties of cow dung fiber from a micro perspective. In this study, an S-4800 cold field emission SEM was used to detect the morphology and phase composition of CDF with different surface treatments, according to its imaging depth and three-dimensional characteristics. In the test, the cow dung fibers were first pasted on the sample plate through conductive double-sided adhesive, the samples were then sprayed with gold, and finally scanned by the SEM. The test voltage is 5 kV, and the magnification is 150 and 200 times respectively.

Thermogravimetric analysis (TGA)

For the evaluation of thermal stability and effects of surface treatment on the composition and structure of cow dung fibers, thermogravimetric (TG) curves of the prepared samples were constructed via a TA Instruments (DSC/TGA Discovery SDT 650). During the testing, 5 mg of samples were heated in a nitrogen atmosphere from 20 to 700 ℃ at a linear heating rate of 20 ℃/min. The mass change, endothermic and exothermic conditions of the samples during heating were then analyzed according to the weight loss results.

Rotational viscosity (RV) test

The viscosity of asphalt binder reflects its ability to resist shear deformation and flow under external pressure. In this study, the viscosity of CDFMA at five temperatures (110 ℃, 120 ℃, 135 ℃, 150 ℃ and 160 ℃) was measured using a Brookfield viscometer. The test was carried out following an AASHTO specification (AASHTO T316-13). The viscosity was measured at a spindle speed of 20 rpm and the corresponding viscosity-temperature curve was plotted.

Table 2 Identifications of asphalt binders

Binder types	Identification
AH-70 asphalt	BA
Blending 1 mm length of ATCDF into AH-70 asphalt	ATCDFMA-1
Blending 2 mm length of ATCDF into AH-70 asphalt	ATCDFMA-2
Blending 1 mm length of STCDF into AH-70 asphalt	STCDFMA-1
Blending 2 mm length of STCDF into AH-70 asphalt	STCDFMA-2
Blending 1 mm length of CDF into AH-70 asphalt	CDFMA-1
Blending 2 mm length of CDF into AH-70 asphalt	CDFMA-2

The temperature sensitivity of CDFMA was evaluated by a viscosity-temperature curve.

Frequency sweep test

Frequency sweep test was used to measure and analyze the rheological response of asphalt samples over a large temperature and frequency range. Strain amplitude sweep tests were undertaken with the strain amplitudes ranging from 0.1 to 30% to determine the linear viscoelastic (LVE) strain range of asphalt binder samples. The strain-controlled frequency sweep tests were then conducted to obtain the samples' complex shear modulus and phase angle at 5 different temperatures (46 ℃, 52 ℃, 58 ℃, 64 ℃, 70 ℃) with frequency varied from 0.1 to 25 Hz. This work focused to reveal the rheological response under the high temperature conditions. We chose 46 ℃ as the lowest temperature.

It is noted that the strain levels were controlled within the viscoelastic strain range. Further, the sigmoidal model was used to obtain the time–temperature shift factors and construct the master curve of complex shear modulus and phase angle based on the time–temperature superposition principle, as shown in Eqs.1 and 2:

$$\alpha(T) = \frac{f_r}{f} \tag{1}$$

$$\log|G^*| = \delta + \frac{\alpha}{1 + e^{\beta+\gamma\log(f_r)}} \tag{2}$$

where α(T) is the shift factor at temperature T relative to the reference temperature, f_r is the reduced frequency at the reference temperature (Hz), f is the frequency at tested temperature (Hz), |G*| is the complex modulus (Pa), and α, δ, β, and γ are model coefficients.

MSCR test

MSCR test (AASHTO T350) was used to evaluate the rutting resistance of each asphalt binder sample at a high temperature. In this test, a loading plate with a diameter of 25 mm and a gap of 1 mm was selected. The MSCR test was carried out on the samples before and after short-term aging (RTFO) at three temperatures (i.e. 64 ℃, 70 ℃ and 76 ℃). During this testing process, the samples were loaded at a constant stress level of 0.1 kPa and 3.2 kPa for 20 and 10 creep-recovery cycles respectively, with each cycle loading for 1 s and recovery for 9 s. The non-recoverable compliance (J_{nr}) and percent recovery (R) of asphalt binders in each creep-recovery cycle were obtained to evaluate their high-temperature rheological properties.

Fatigue tests of cow dung fiber-modified asphalt

The fatigue test mainly included two parts in this study. In the first portion, the LAS test in AASHTO TP 101 was used to evaluate the fatigue life of asphalt samples with long-term aging (PAV). The accelerated fatigue damage tests on asphalt specimens were performed through a DSR device at 20 ℃ under a loading frequency of 10 Hz. The amplitude of the loading oscillating shear strain increased linearly from 0.1 to 30%. The fatigue equation is as follows:

$$N_f = A\,(\gamma_P)^{-B} \tag{3}$$

where N_f represents the fatigue life;γ_p is the applied amplitude shear strain; A, B and S_f are the fitting parameters, which are expressed by Eqs. 4, 5 and 6, respectively (Sun et al. 2019).

$$A = \frac{f\,S_f^{1+\alpha(1-C_2)}}{\left[1+\alpha(1-C_2)\right]\left(\frac{1}{2}C_1\,C_2\right)^{\alpha}\left(|G*|_{LVE}\right)^{2\alpha}} \tag{4}$$

$$B = 2\alpha \tag{5}$$

$$S_f = \left(\frac{1-C_f}{C_1}\right)\frac{1}{C_2} \tag{6}$$

where f is the reduced frequency; S_f is the damage accumulation corresponding to the fatigue failure point; C_f refers to the material integrity corresponding to the point at peak stress; and C_1 and C_2 are fitting coefficients.

In the second portion, time sweep test was performed to evaluate the fatigue performance of PAV asphalt specimens. Parallel loading plates with a diameter of 8 mm (gap of 2 mm) were used in this test. The samples were loaded for 54,000 cycles at a temperature of 20 ℃, a frequency of 10 Hz and a strain amplitude of

5% to determine the complex shear modulus and phase angle of the samples under failure damaged conditions. The fatigue crack length of asphalt samples after failure can be obtained by digital image processing and DSR-C model.

The DSR-C model described in Eq. 7 was established by Zhang and Gao based on the balance principle of torque and dissipative strain energy of viscoelastic damage mechanics, which has been employed to calculate the crack length of various asphalt binders under the rotational shear fatigue load (Gao et al. 2020a, 2020b; Yga et al. 2021; Zhang and Gao 2019).

$$c = \left[1 - \left(\frac{\left|G_N^*\right| / \sin\left(\delta_N\right)}{\left|G_0^*\right| / \sin\left(\delta_0\right)}\right)^{\frac{1}{4}}\right] r_0 \tag{7}$$

where c is the crack length of asphalt samples; r_o is the original radius of asphalt samples; $\left|G_0^*\right|$ and δ_0 represent the dynamic modulus and phase angle of asphalt in undamaged state; $\left|G_N^*\right|$ and δ_N represent the dynamic modulus and phase angle of asphalt under the N-th cyclic loading.

Results and discussion

Surface morphology of cow dung fibers

Figure 3 shows the SEM results of CDF before and after pretreatment. It can be seen from the SEM micrographs that the surface of CDF is smooth and uniform and they are closely arranged (Fig. 3a), which is not conducive to dispersion. By contrast, the surface texture of STCDF turns out to be rough

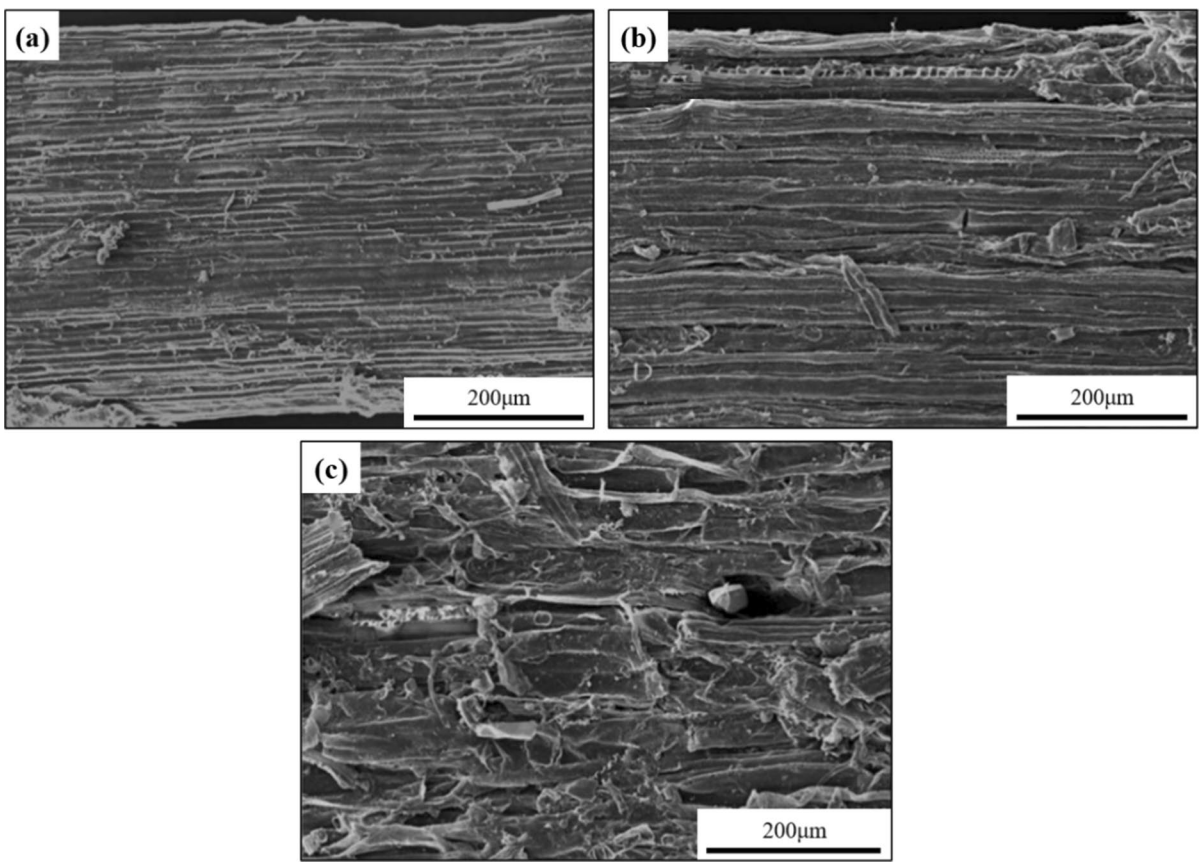

Fig. 3 SEM image of the cow dung fiber surface: **a** CDF; **b** STCDF; **c** ATCDF

and is coated with a layer of reagent due to the silane coupling agent (Fig. 3b). When the cow dung fiber is processed with alkaline solution and silane coupling agent, it can be observed that the solvent coating on the ATCDF surface is more pronounced and more grooves appear (Fig. 3c). This is attributed to the fact that alkali pretreatment dissolves impurities in cow dung fibers, including hemicellulose and lignin, and breaks the hydrogen bonds between cellulose molecules (Gholampour and Ozbakkaloglu 2019), resulting in a rough surface morphology of the fibers. Furthermore, the presence of grooves increases the contact area between ATCDF and coupling agent, causing more solvent to be adsorbed on the surface and eventually resulting in better interfacial adhesion to the asphalt binder matrix. From this point of view, STCDF and ATCDF will possess a better modification due to the existence of surface coupling agent reagent layer that strengthens the combination of fiber and asphalt.

Thermal stability of cow dung fibers

Figure 4 presents the variational residual weight percentage and mass loss rate of three cow dung fibers in the temperature range of 20–700℃. It can be seen from the TG curves in Fig. 4a that CDF, STCDF and ATCDF exhibit similar thermal degradation trend, which can be divided into three stages. The mass loss in the first stage is between 20℃ and 200℃, which is attributed to the evaporation of free water and chemically bound water in the cow dung fibers (Jones et al. 2018). It can be clearly seen that the starting and ending decomposition temperatures of the three fibers at this stage are almost the same and the fraction of thermal weight loss is less than 10%, indicating that alkali treatment and surfactant treatment applied in this research have no significant effect on the existence of water in the structure of cow dung fibers. In other words, the effects of alkali treatment and interfacial coupling treatment on fibers composition could be negligible within the temperature range for the preparation of modified asphalt.

The second decomposition stage occurs in the temperature range of 200–400 ℃. At this stage, the macromolecular components such as cellulose, lignin and hemicellulose in fibers are pyrolyzed (Bradbury et al. 2010). This process is the most obvious thermal weight loss stage in the TG curves due to the high

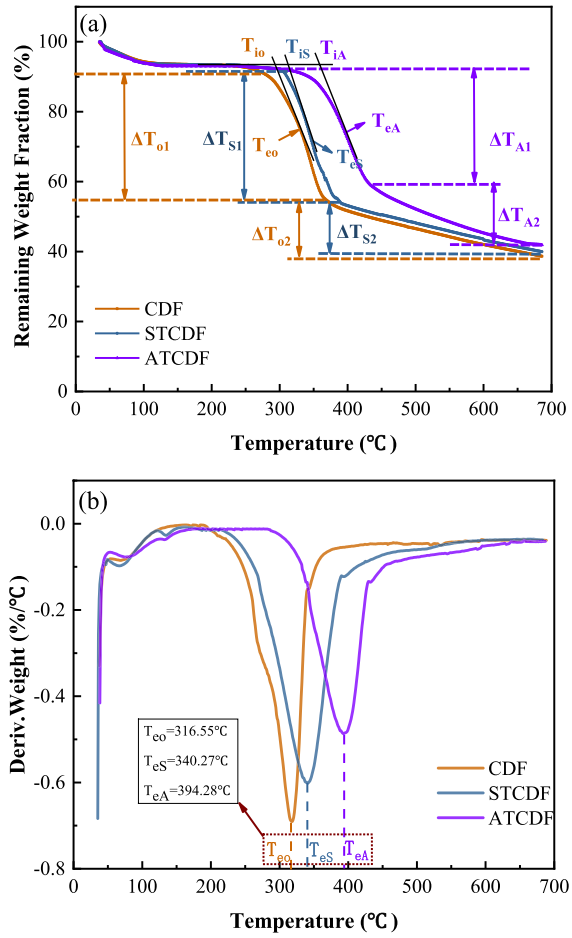

Fig. 4 TG test results of cow dung fibers with different treatment methods: **a** TG curves; **b** Differential thermogravimetric (DTG) curves

content of these macromolecules in the cow dung fiber structure. In order to accurately determine the starting and ending decomposition temperatures of the mass loss stage, the time coordinates of each point on the TG curves were differentiated to obtain the differential thermogravimetric (DTG) curve, as shown in Fig. 4b, which characterizes the variation of the weight change rate with temperature. The peak point is the temperature point with the largest mass change rate in the TG curve (inflection point). It can be seen from Fig. 4b that the peak temperature of CDF is 316.55 ℃ (T_{eo}), while the peak temperatures of STCDF (T_{eS}) and ATCDF (T_{eA}) appear at 340.27 ℃ and 394.28 ℃, respectively. In TG curves, the tangent line at the peak DTG temperature of the three fibers intersects the tangent line at the platform before

decomposition reaction, which is the initial reference temperature (T_{io}, T_{iS}, T_{iA}) for decomposition reaction. As seen from Fig. 4a, the initial pyrolysis temperature of CDF and STCDF is 300–400 ℃, which indicates that the pyrolysis of cellulose and hemicellulose mainly occurs in this decomposition stage. By comparison, the initial pyrolysis temperature of ATCDF is higher than 350 ℃, with this exceeding the decomposition temperature of hemicellulose. Therefore, the main pyrolysis component is cellulose. This can be attributed to the fact that alkali treatment dissolves hemicellulose from the cow dung fibers (Gholampour and Ozbakkaloglu 2019).

When the temperature is higher than 400 ℃, the small molecules generated at the second stage of decomposition are further decomposed, which is the residual decomposition stage. The small molecule obtained from macromolecules such as hemicellulose, which are dissolved by an alkaline solution. The thermal weight loss range at this stage is relatively small. TG curves reveal that CDF and STCDF have similar thermal weight loss, while ATCDF has greater thermal weight loss, proving a higher proportion of small molecule mass in ATCDF.

Rotational viscosity

The viscosity of the samples was determined by a Brookfield viscometer with a temperature control device. The test results of cow dung fiber modified asphalt with different lengths and treatment methods were shown in Fig. 5. The viscosity of the binders exhibits a nonlinear attenuation trend with the increasing temperature. It is noteworthy that CDFMA with different lengths of cow dung fibers have a higher viscosity than BA in the selected temperature range, indicating that the addition of CDF increases the viscosity significantly.

In addition, it is seen that the viscosity of CDFMA-2 is higher than that of CDFMA-1, especially in the range of 110–120 ℃ and after surface treatment. The results suggest that the increase of cow dung fiber length can increase the viscosity, which can be attributed to the more remarkable fiber network. Moreover, the two kinds of surface treatments can further improve reinforcing effect of the fiber network.

In terms of asphalt binders modified by CDF, STCDF and ATCDF, it can be observed that

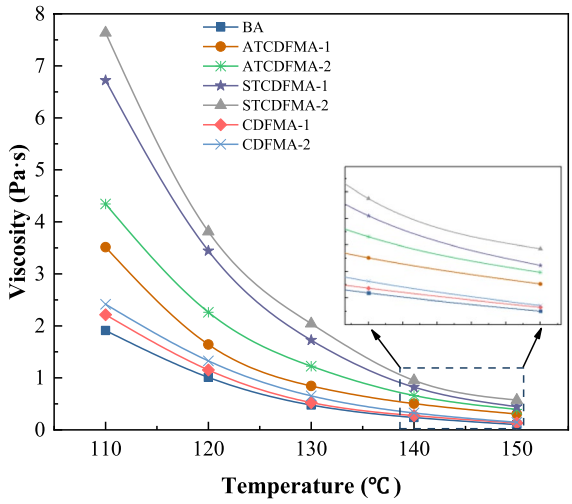

Fig. 5 Viscosity versus temperature curve of asphalt binders

STCDFMA exhibited the highest viscosity, followed by ATCDFMA, and CDFMA has the lowest viscosity under a condition of constant fiber length. The reason is that the compatibility between the CDF and the asphalt is improved by surface treatment, which facilitates the formation of three-dimensional (3D) network structure in the asphalt binder. The interlacing and winding effects between fibers become more evident, making CDFMA more viscous. By contrast, the ATCDFMA obtained by alkali treatment has a lower viscosity than STCDFMA due to the degradation reaction of hemicellulose and lignin, which reduces its polymerization degree and weakens the network structure of CDF.

The quantitative relationship between viscosity and temperature can be analyzed using Saal's formula (Wang et al. 2014), as expressed in Eq. (8).

$$\lg(\lg \eta \times 10^3) = n - m \lg(T + 273) \tag{8}$$

where η represents the kinematic viscosity; T represents the temperature; m is the regression coefficient, its absolute value characterizes the temperature sensitivity of the material within the tested temperature range; and n represents a constant relating to the physical properties of the fluid. The Saal formula was used to process the data and the double-logarithmic viscosity-temperature curves were obtained, as shown in Table 3 and Fig. 6. According to the viscosity-temperature sensitivity (VTS) method, the smaller

Table 3 Regression analysis of double logarithmic viscosity versus temperature curve of asphalt binders

Asphalt type	Regression equation*	Correlation coefficient (R^2)
BA	$y_1 = 13.156 - 4.889x$	0.9769
ATCDFMA-1	$y_2 = 9.753 - 3.563x$	0.9988
ATCDFMA-2	$y_3 = 9.389 - 3.417x$	0.9988
STCDFMA-1	$y_4 = 10.244 - 3.738x$	0.9946
STCDFMA-2	$y_5 = 9.624 - 3.496x$	0.9955
CDFMA-1	$y_6 = 12.408 - 4.597x$	0.9893
CDFMA-2	$y_7 = 12.101 - 4.475x$	0.9774

*y represents lg (lg $\eta \times 10^3$) and x represents lg (T + 273)

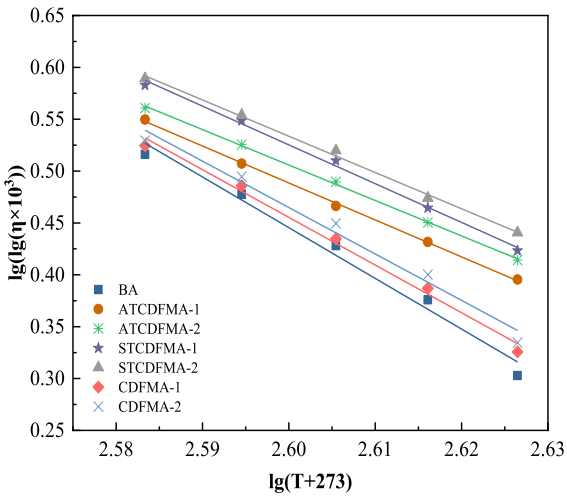

Fig. 6 Double-logarithmic viscosity versus temperature curve of asphalt binders

the absolute value of viscosity-temperature index, the less sensitivity of asphalt to temperature. It can be seen from the regression fitting results that the temperature sensitivity of CDFMA is weaker than that of BA. The temperature sensitivity of CDFMA can be inhibited by the two surface pretreatment processes. The ATCDFMA exhibits the least sensitivity to temperature. Furthermore, with an increase in the length of CDF, the high temperature stability of CDFMA is proved to be significantly improved.

Complex modulus and phase angle of CDFMA

Black space diagram

A black space diagram is a graph plotting complex shear modulus versus phase angle obtained from the frequency sweep tests at different temperatures. This representation of the test data eliminates the test parameters (frequency and temperature) and enables the viscoelastic responses of bituminous materials to be analyzed without performing the time–temperature superposition principle (TTSP) manipulations of the raw dynamic data. Generally, the black diagram has been widely used in identifying possible discrepancies in the measurements, in verifying the thermo-rheological simplicity of the different types of binders and time–temperature equivalency, which can be indicated by a smooth curve (Wang et al. 2018).

Figure 7 shows the black space diagram of BA and CDFMA samples in the test temperature and frequency range. It can be clearly seen that the dynamic data of all the binders produced relatively smooth curves with slight scattering. This indicates that BA and CDFMA binders can be considered as thermo-rheological simple materials. Compared with BA, the rheological data of ATCDFMA-1, STCDFMA-1 and CDFMA-1 have a similar trend, but with a shifting towards a lower phase angle (left), which means more elastic behavior. This can be interpreted as the obstruction of cow dung fiber to the viscous flow of asphalt binders. Unlike the black space diagram

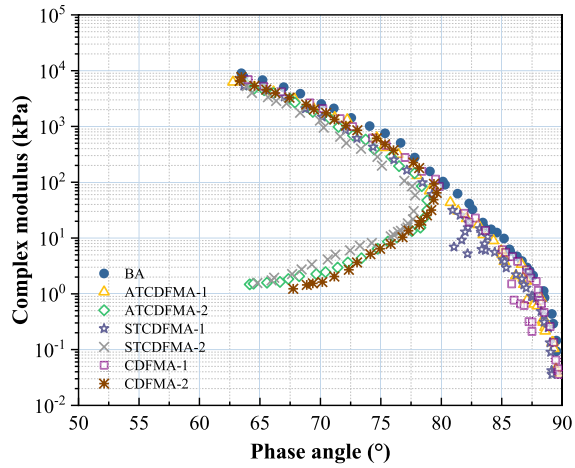

Fig. 7 Black space diagram of BA and CDFMA binders

of samples mentioned above, the curves of ATCDFMA-2, STCDFMA-2 and CDFMA-2 exhibit an inverse "C" pattern, which is similar to the rheological curve of SBS modified asphalt reported in the previous literature (Wang et al. 2018). At a moderate temperature (i.e. 46 ℃, 52 ℃), the curves of ATCDFMA-2, STCDFMA-2 and CDFMA-2 exhibit a similar trend to that of BA because the rheological behavior of the three CDFMA is dominated by the linear viscoelastic response of asphalt matrix in this temperature range. However, these samples have a trend of decreasing phase angle at high temperature (i.e. 58 ℃, 64 ℃ and 70 ℃) as the network reinforced structure formed by fibers with a length of 2 mm controls the rheological response of binders, which increases the friction between asphalt molecules and resists the viscous flow of the asphalt matrix. In addition, the difference of black diagram curves of ATCDFMA, STCDFMA and CDFMA demonstrates that STCDF possesses the most obvious hindrance effect on the viscous flow of asphalt matrix, followed by ATCDF, and CDF.

Master curve

The master curves of complex modulus at the reference temperature of 46℃ are presented in Fig. 8. It can be seen that the increasing reduced frequency led to an upward shift of complex modulus. Moreover, the addition of cow dung fiber is able to provoke a slight increase in the complex modulus of the asphalt binder samples. This means that CDFMA has a higher stiffness at the same temperature and frequency range. By comparison, the samples ATCDFMA and STCDFMA exhibit a higher complex modulus than CDFMA due to the presence of silane coupling agent. It is worth noting that after the alkali treatment, STCDFMA becomes softer based on the fact that ATCDFMA has a lower complex modulus, indicating that alkali treatment has a negative effect on the ability of CDFMA to resist shear loading. This is because that the structural macromolecules in the cow dung fibers are dissolved and destroyed by the alkaline solution, causing a decrease in stiffness. In addition, it can be observed from the master curves of all the CDFMA samples that the increase in the length of the cow dung fibers can slightly enhance the stiffness of the asphalt binders.

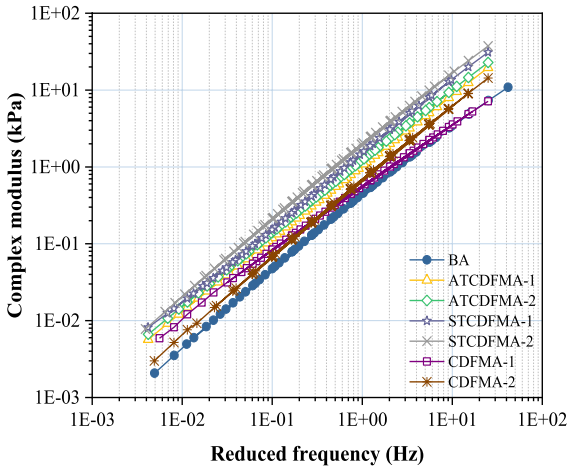

Fig. 8 Master curves of complex modulus for BA and CDFMA binders

MSCR test results

The rutting resistance potential of the RTFO-aged binder samples was characterized by the MSCR test according to AASHTO MP 19, the results were as shown in Fig. 9. The elastic property and permanent deformation resistance of the asphalt binder specimens were evaluated by percent recovery (R) and non-recoverable creep compliance (Jnr) respectively, which can be calculated by Eqs. (9) and (10):

$$R = \frac{\varepsilon_{\mathrm{p}} - \varepsilon_u}{\varepsilon_p} \times 100\% \tag{9}$$

$$Jnr = \frac{\varepsilon_u}{\sigma} \tag{10}$$

where ε_p is the peak strain in creep stage; ε_u is the unrecovered strain in a creep-recovery cycle; and σ is the stress level (kPa) applied during creep phase. The average percent recovery and non-recoverable creep compliance of binders in 10 creep recovery cycles at 0.1 and 3.2 kPa stress level were expressed as $R_{0.1}$, $R_{3.2}$, $Jnr_{0.1}$ and $Jnr_{3.2}$, respectively. The stress sensitivity indexes of R_{diff} and Jnr_{diff} are calculated according to Eqs. (11) and (12) respectively:

$$R_{\mathrm{diff}} = [(R_{0.1} - R_{3.2})/R_{0.1}] \times 100\% \tag{11}$$

$$Jnr_{diff} = [(Jnr_{3.2} - Jnr_{0.1})/Jnr_{0.1}] \times 100\% \tag{12}$$

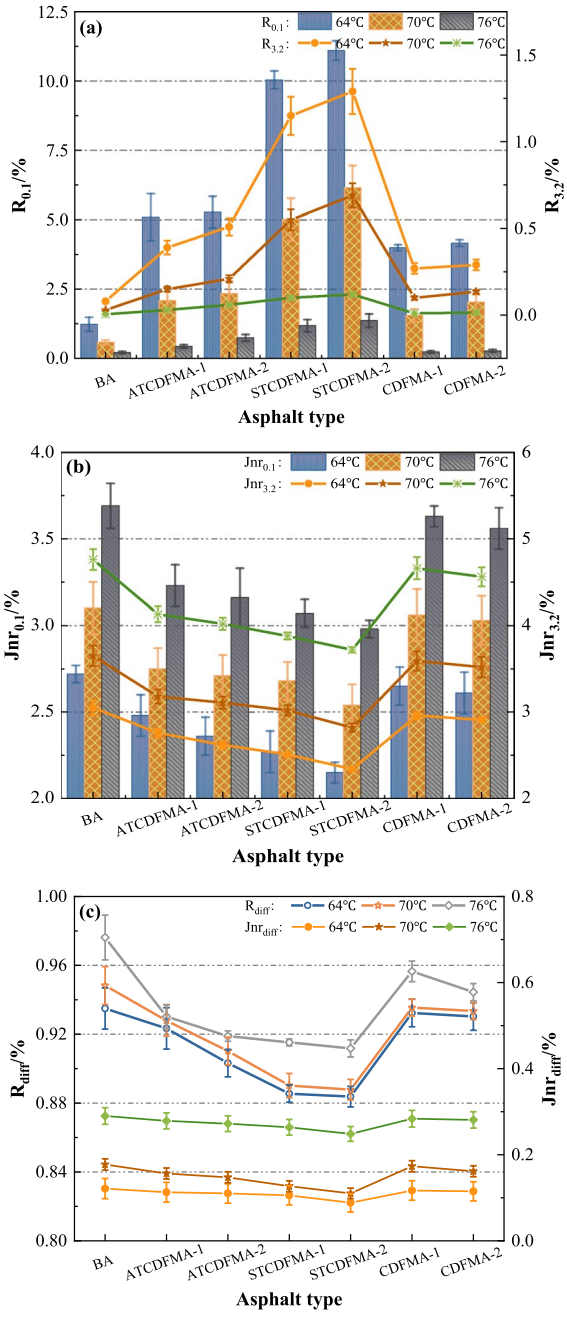

Fig. 9 MSCR parameters for all the RTFO-aged samples at 64 °C, 70 °C and 76 °C: **a** R0.1 and R3.2; **b** Jnr0.1 and Jnr3.2; **c** Rdiff and Jnrdiff

According to Fig. 9a, b, compared with BA, all the CDFMA samples exhibit lower non-recoverable creep compliance with higher percent recovery, which means a better resistance to rutting deformation. This demonstrates that the presence of cow dung fibers inhibit the generation of irreversible deformation of asphalt binder. Among the three types of CDFMA samples, STCDFMA shows the most desirable MSCR parameters, followed by ATCDFMA, while CDFMA possesses the largest Jnr and the smallest R value. This phenomenon proved that surface coupling pretreatment has an enhancement effect on creep deformation recovery and rutting resistance of CDFMA, but alkali treatment attenuated this enhancement due to the destruction of cow dung fiber structure by alkali. Furthermore, it can be noted that the rutting resistance of CDFMA-2 is superior to that of CDFMA-1. The main reason accounting for this is that long fiber is more likely to form a network reinforcement structure in asphalt binder, improving the deformation resistance. In addition, it's worth noting that the difference of MSCR parameter values of all the samples is diminished with the increase of temperature, indicating that the deformation resistance of cow dung fibers is weakened at high temperature (i.e. 76 ℃).

Figure 9c illustrates the stress sensitivity indexes results of BA and CDFMA. It can be seen that both the increase in fiber length and the surface coupling treatment reduce the stress sensitivity for R and Jnr of CDFMA. R_{diff} and Jnr_{diff} exhibit similar sensitivity to high-temperature as R and Jnr.

Fatigue characteristics of CDFMA

LAS test results

Figure 10 presents the stress–strain curves for PAV-aged binder samples from LAS tests. It can be seen that the shear stress response of all asphalt binders exhibited distinct peaks but appeared at different strains, which is called the yield stress (strength) of the material. The shear strain corresponding to the yield stress is the yield strain. After the peak, a substantial drop in shear stress can be observed, indicating that significant damage to the specimen has occurred. Obviously, the yield strains of all the CDFMA are higher than BA except for CDFMA-1, which demonstrates that the addition of CDF accelerates the destruction, but the failure of binders could be hindered by pretreatment on the fiber surface or increasing the fiber length. In addition, compared to

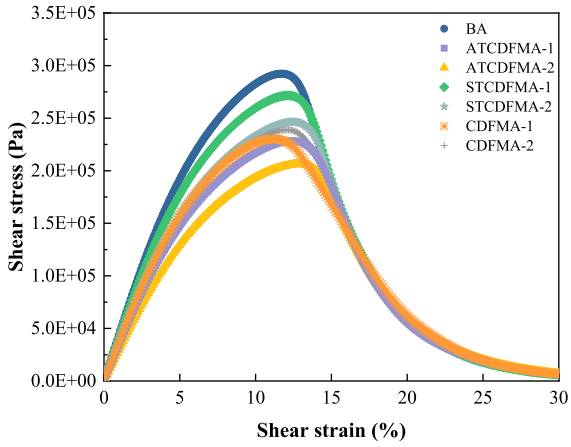

Fig. 10 Stress–strain curves from the LAS test for PAV-aged asphalt binders

BA, all the CDFMA binders show lower maximum stress values, which suggests that the addition of cow dung fiber leads to a decrease in the stiffness of the asphalt binder.

With the VECD theory based on pseudo strain energy (PSE) (Park et al. 1996), the relationship between damage strength S and material integrity C can be quantified, and the results are shown in Fig. 11. At constant damage density, binders with higher C values possess better fatigue resistance, indicating higher material integrity under load cycles. As seen from the curves that there is no significant difference in C values of BA and CDFMA when the damage intensity is low. As the S increases, it is evident that the addition of cow dung fiber enables the asphalt binder to present a small decline of C when bearing the same level of damage, which demonstrates a better fatigue performance. However, the improvement of the fatigue resistance of BA by the six fibers occurs at different damage densities. ATCDFMA and STCDFMA show higher durability at smaller damage densities, while CDFMA-1 at higher damage densities (over 150).

Figure 12 illustrates the predicted fatigue lives for the binders through VECD theory at the two applied strain levels. It can be seen that fatigue lives of all the binders decreases with strain level increases and the fatigue resistance of BA displays the worst at any strain amplitude. Obviously, the addition of cow dung fibers considerably enhances the fatigue life of BA. Besides, it can be found from the fatigue life of CDFMA samples that both the pretreatment and the increase in fiber length could enhance the durability of asphalt binders, especially the pretreatment by a combination of alkali and coupling agent. For instance, the ATCDFMA-2 affords the fatigue lives 1.14, 1.27 and 1.12 times longer than STCDFMA-2, CDFMA-2 and STCDFMA-1 at the strain amplitudes of 2.5%, respectively. The cause is that ATCDF bonds more tightly with the asphalt matrix and its higher interface energy effectively prevents the expansion of fatigue cracks. On the other hand, the increased fiber length enhances bridging effects and thus inhibits crack growth.

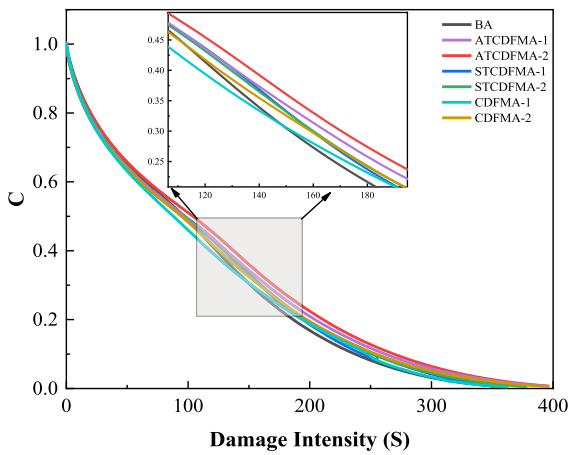

Fig. 11 Relationship between parameter C and damage density of PAV-aged asphalt binders

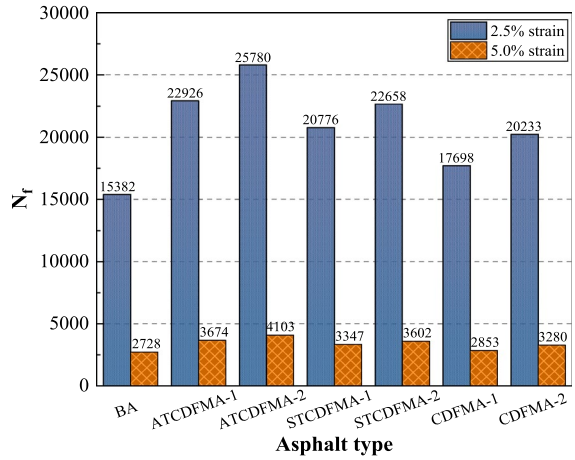

Fig. 12 Predicted fatigue lives for PAV-aged asphalt binders at 2.5% and 5.0% strain amplitudes

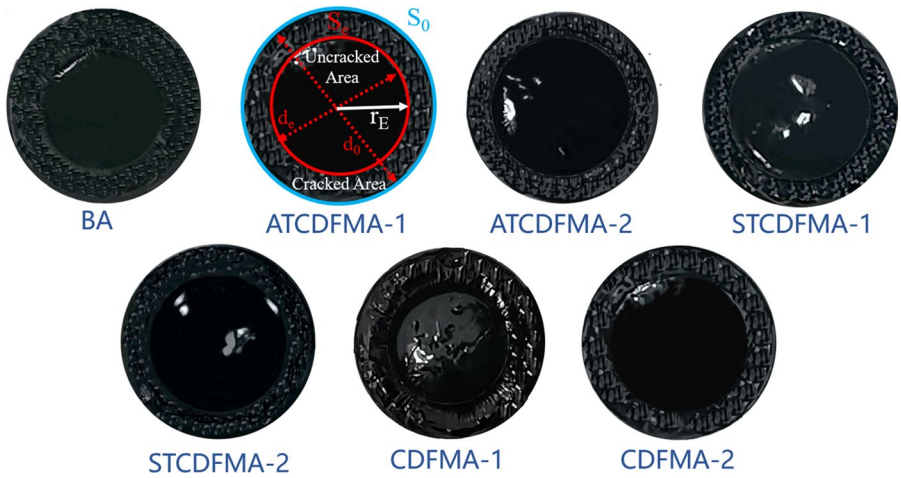

Fig. 13 Images of cracking surfaces for asphalt binders after time sweep tests at 20 °C and 10 Hz

Time sweep test results

A typical image of asphalt cracking surface after the time sweep fatigue test is presented in Fig. 13. From the images it can be observed that the asphalt sample surface displays distinct morphology in different areas. In the central region of the specimen, the surface is flat and smooth, which represents the uncracked part of the specimen during the time sweep test. In the edge region of the specimen, a circular rough surface consisting of radial peaks and valleys (referred to as the "factory roof") is fatigue crack area caused by the interaction between the surface and the bottom of the specimen triggered by the shear load.

The surface morphology of ATCDFMA-1 is labelled to show how the fatigue crack length is obtained from the asphalt cracking surface photos. Firstly, the boundary between the undamaged area and the cracked area is marked out using Adobe Photoshop CS6 software based on the noticeable difference in grayscale values. The pixel area statistics function in the Image Pro Plus (IPP) 6.0 software is then used to calculate the pixel area of the undamaged area and the whole sample area and replace the actual area ratio with the pixel area ratio (S_e/S_0). The final crack length (c), denoted as the measured crack length, can be obtained by Eq. (13):

$$c = \frac{d_0(1 - \sqrt{S_e/S_0})}{2} \tag{13}$$

where d_0 is the diameter of the asphalt sample, 8 mm.

In the DSR-C model, the crack length of asphalt during time sweep testing is predicted from the complex shear modulus and phase angle of the specimen under undamaged and damaged conditions, as shown in Eq. (7). The complex shear modulus ($|G_0^*|$) and phase angle (δ_0) in the undamaged condition can be obtained from the frequency sweep test in LAS test. The shear modulus ($|G_N^*|$) and the phase angle (δ_N) with the 54,000th load cycles under the damaged condition are obtained by the time sweep tests. Taking CDFMA-1 as an example, the process of obtaining the above parameters is shown in Fig. 14.

The results of measured crack length and calculated crack length obtained by DSR-C model are presented in Table 4. It can be seen that the crack length values of all the CDFMA samples are smaller than that of BA, indicating that the addition of cow dung fiber can improve the fatigue resistance of asphalt binders. Besides, the variations in the crack lengths of the six CDFMAs exhibit a good concordance with the results of their fatigue life from the LAS test. This further proves the pretreatment and increased fiber length enhance the durability of asphalt. In addition, the cow dung fiber modified by a combination of alkali and silane coupling agent is more effective in preventing fatigue cracking of the asphalt binder, demonstrated by the minimum crack length values.

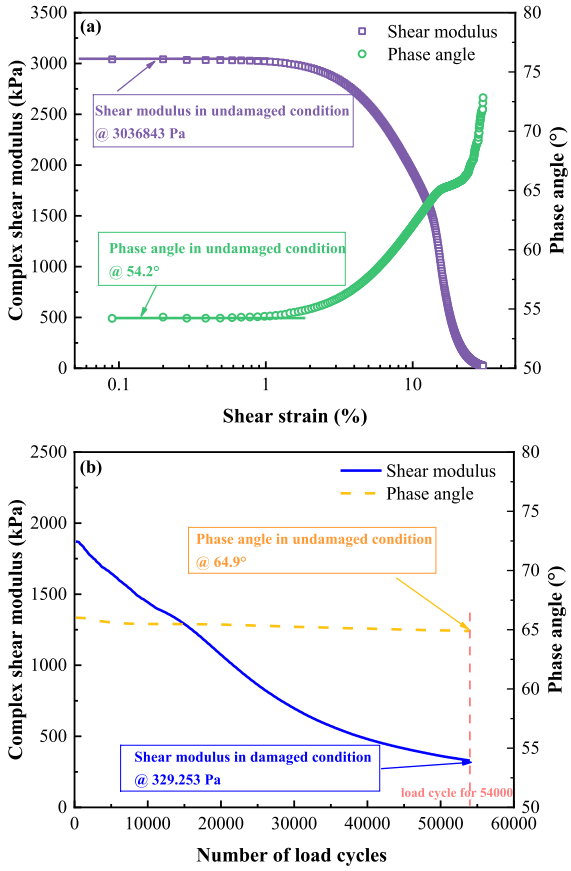

Fig. 14 Results of LAS test and time sweep test for CDFMA-1: **a** Shear modulus and phase angle in undamaged condition; **b** Shear modulus and phase angle in damaged condition

Comparison of DSR-C model and fatigue parameter N_f

Figure 15a presents the comparison between the calculated crack length obtained from the DSR-C model and the measured results. The quality line (y = x) is added to visualize the difference between the theoretical and actual results. The proximity of the data points to the quality line can be measured by sum squared residuals (SSR). It is found that the predicted crack length agrees well with the actual measured values with an SSR of 0.05, which verifies the accuracy of the DSR-C model in terms of fatigue performance prediction of asphalt binders. Furthermore, the fitting curve of the fatigue life (N_f) obtained in the LAS tests versus the measured crack length from time sweep tests at 5% strain level was plotted in Fig. 15b. It can be seen that its correlation coefficient R value of N_f is 0.87, which is smaller than that (0.97) of the DSR-C model shown in Fig. 15a. This indicates that the DSR-C model presents a more accurate fatigue resistance evaluation of asphalt binders than that of the fatigue parameter N_f obtained from the LAS tests. The reason is because that the variation range of strain amplitude in the LAS tests is too large. When the strain level exceeds the yield strain of the material, the asphalt specimen will be damaged in advance. The damage at this point is caused by the too large strain level rather than fatigue. Overall, the DSR-C model is capable of accurately evaluating the fatigue resistance of the CDFMA.

Conclusions

In this study, the rheological and fatigue characteristics of cow dung fiber-modified asphalt binders were investigated with the effects of surface treatment and fiber length. The surface morphology and thermal stability of cow dung fibers with surface coupling

Table 4 Calculation results of fatigue crack in asphalt binders

Samples	G_0^*(kPa)	δ_0(°)	G_N^*(kPa)	δ_N(°)	Calculated crack length(mm)	Measured crack length(mm)
BA	2845.645	57.32	285.219	64.02	1.786057	1.767074143
ATCDFMA-1	3781.386	55.21	697.572	65.70	1.445927	1.494999859
ATCDFMA-2	4254.973	54.63	829.521	63.07	1.400762	1.436775888
STCDFMA-1	3700.768	55.38	517.533	64.77	1.611065	1.597196609
STCDFMA-2	3768.360	54.69	672.349	64.00	1.462311	1.536222377
CDFMA-1	3036.843	54.57	329.253	64.90	1.764511	1.703233404
CDFMA-2	3515.325	54.24	511.650	64.69	1.595141	1.649942055

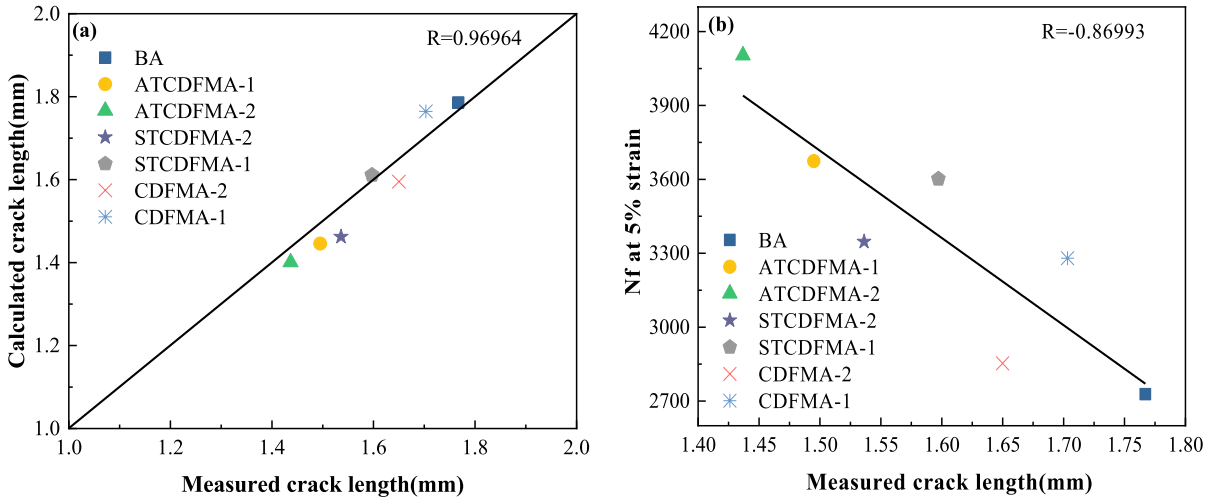

Fig. 15 Fatigue performance prediction of asphalt binders based on DSR-C model and fatigue parameter Nf: **a** Comparison between calculated and measured crack length in time sweep tests at the 54000th load cycles; **b** Comparison between fatigue life obtained in LAS tests and measured crack length

treatment, alkali treatment and two fiber lengths were first measured using SEM and TG. The viscosity test, frequency sweep test and MSCR test were performed to evaluate the rheological properties of CDFMA with different lengths and surface treatments. The fatigue properties of CDFMA were characterized by LAS and time sweep tests. Based on the results and analysis, the following conclusions can be drawn:

(1) The surface treatment increases the roughness of the cow dung fiber surface, which covers the surface with a solvent layer and facilitates the compatibility of asphalt binders and cow dung fiber.
(2) The surface coupling treatment of cow dung fibers increases the stiffness of asphalt binders. The fiber length has no significant effect on the stiffness of the binders.
(3) CDFMA-1, STCDFMA-1 and ATCDFMA-1 can be considered as thermo-rheological simple materials. The master curves of three CDFMAs modified with 2 mm fibers show an inverse "C" pattern.
(4) The surface treatments and the increase in fiber length can improve the high-temperature permanent deformation resistance of asphalt binders. STCDFMA-2 exhibits the best high-temperature performance among all seven binders.
(5) ATCDFMA shows the highest fatigue cracking resistance, followed by STCDFMA and finally CDFMA. The increase in fiber length slightly inhibited the fatigue cracking.
(6) Compared to the index of fatigue life N_f, the fatigue crack length of CDFMA calculated by the DSR-C model correlated better with the measured results from time sweep fatigue tests.

Author contributions DN: Methodology, Data analysis, Results discussion, Supervision, Writing–review and editing, Validation. ZZ: Investigation, Testing, Data analysis, Result discussion, Writing–original draft. YG: Methodology, Investigation, Validation, Supervision. YL: Resources, Investigation, Validation. ZY: Investigation, Validation, Supervision. YN: Writing–review and editing, Supervision.

Funding This study was sponsored by Science and Technology Project of Housing and Urban Rural Development Department of Shaanxi Province (2020-K11), European Union's Horizon 2020 research and innovation programme under the Marie Skłodowska-Curie grant agreement (No. 101030767), the Special Fund for Basic Scientific Research of Central Colleges (No. 300102310301). The authors gratefully acknowledge their financial support.

Data availability The datasets used or analyzed during the current study are available from the corresponding author on reasonable request.

Declarations

Conflict of interest The authors declare that they have no known competing financial interests or personal relationships that could have appeared to influence the work reported in this paper.

References

Adeyi AJ, Adeyi O, Oke EO, Olalere OA, Oyelami S, Ogunsola AD (2021) Effect of varied fiber alkali treatments on the tensile strength of ampelocissus cavicaulis reinforced polyester composites: prediction, optimization, uncertainty and sensitivity analysis. Adv Ind Eng Polym Res 4:29–40. https://doi.org/10.1016/j.aiepr.2020.12.002

Ananno AA, Masud MH, Mahjabeen M, Dabnichki P (2021) Multi-utilisation of cow dung as biomass. In: Inamuddin AK (ed) Sustainable bioconversion of waste to value added products. Springer International Publishing, Cham, pp 215–228. https://doi.org/10.1007/978-3-030-61837-7_13

Aravinth K, Ramakrishnan T, Tamilarasan VD, Veeramanikandan K (2022) A brief review on plant fibres composites: extraction, chemical treatment and fibre orientation. Mater Today Proc. https://doi.org/10.1016/j.matpr.2022.02.291

Bradbury A, Sakai Y, Shafizadeh F (2010) A kinetic model for pyrolysis of cellulose. J Appl Polym Sci 23:3271–3280. https://doi.org/10.1002/app.1979.070231112

Bridget T, Bello ZA, Ololade OO (2020) Comparative nutrient leaching capability of cattle dung biogas digestate and inorganic fertilizer under spinach cropping condition. Environ Sci Pollut Res 27:3237–3246. https://doi.org/10.1007/s11356-019-07104-8

Brugnago RJ, Satyanarayana KG, Wypych F, Ramos LP (2011) The effect of steam explosion on the production of sugarcane bagasse/polyester composites. Compos Part A Appl Sci Manuf 42:364–370. https://doi.org/10.1016/j.compositesa.2010.12.009

Chen Z, Yi J, Chen Z, Feng D (2019) Properties of asphalt binder modified by corn stalk fiber. Constr Build Mater 212:225–235. https://doi.org/10.1016/j.conbuildmat.2019.03.329

Chen H, Wu J, Shi J, Zhang W, Wang H (2021) Effect of alkali treatment on microstructure and thermal stability of parenchyma cell compared with bamboo fiber. Ind Crops Prod 164:113380. https://doi.org/10.1016/j.indcrop.2021.113380

Dongjin W, Lairong W, Yongde L, Hailiang Z, Jun F, Shuhu X (2018) Adsorption of low concentration perchlorate from aqueous solution onto modified cow dung biochar: effective utilization of cow dung, an agricultural waste. Sci Total Environ 636:1396. https://doi.org/10.1016/j.scitotenv.2018.04.431

Elo A, Yz A, Fan GA, Tao MB, Ph C, Rong LD (2020) Rheological and fatigue characterisation of bitumen modified by anti-ageing compounds. Constr Build Mater 265:120307. https://doi.org/10.1016/j.conbuildmat.2020.120307

Gao Y, Li L, Zhang Y (2020a) Modelling crack propagation in bituminous binders under a rotational shear fatigue load using Pseudo J-integral Paris' Law. Transp Res Rec J Transp Res Board 2674:036119811989915. https://doi.org/10.1177/0361198119899151

Gao Y, Li L, Zhang Y (2020) Modelling crack initiation in bituminous binders under a rotational shear fatigue load. Int J Fatigue. https://doi.org/10.1016/j.ijfatigue.2020.105738

Gholampour AA, Ozbakkaloglu T (2019) A review of natural fiber composites: properties, modification and processing techniques, characterization, applications. J Mater Ence 55:829–892. https://doi.org/10.1007/s10853-019-03990-y

Gupta KK, Aneja KR, Rana D (2016) Current status of cow dung as a bioresource for sustainable development. Bioresour Bioprocess 3:1–11. https://doi.org/10.1186/s40643-016-0105-9

Hendarto E, Suwarno S, Sudiarto P (2019) Influence of urea-dairy cattle dung fertilizer combinations on growth and production of mulato grass (Brachiaria Hybrid cv "Mulato"). Animal Prod 20(1):29. https://doi.org/10.20884/1.jap.2018.20.1.686

Hintz C, Bahia H (2013a) Simplification of linear amplitude sweep test and specification parameter. Transp Res Rec J Transp Res Board 2370:10–16. https://doi.org/10.3141/2370-02

Hintz C, Bahia H (2013b) Understanding mechanisms leading to asphalt binder fatigue in the dynamic shear rheometer. Road Mater Pavement Des 14:231–251. https://doi.org/10.1080/14680629.2013.818818

Hl A, Zf A, Ata B, My A, Cc A, Gz A, Ping GC, Ys B (2022) Repurposing waste oils into cleaner aged asphalt pavement materials: a critical review. J Clean Prod 334:130230. https://doi.org/10.1016/j.jclepro.2021.130230

Huda MS, Drzal LT, Mohanty AK, Misra M (2008) Effect of fiber surface-treatments on the properties of laminated biocomposites from poly(lactic acid) (PLA) and kenaf fibers. Compos Sci Technol 68:424–432. https://doi.org/10.1016/j.compscitech.2007.06.022

Iwuozor KO, Emenike EC, Aniagor CO, Iwuchukwu FU, Ibitogbe EM, Okikiola TB, Omuku PE, Adeniyi AG (2022) Removal of pollutants from aqueous media using cow dung-based adsorbents. Curr Res Green Sustain Chem 5:100300. https://doi.org/10.1016/j.crgsc.2022.100300

Jones M, Bhat T, Kandare E, Thomas A, Joseph P, Dekiwadia C, Yuen R, John S, Ma J, Wang CH (2018) Data: Thermal degradation and fire properties of fungal mycelium and

mycelium-biomass composite materials. Sci Rep. https://doi.org/10.1515/9783035608922-017
Li L, Gao Y, Zhang Y (2021) Fatigue cracking characterisations of waste-derived bitumen based on crack length. Int J Fatigue 142:105974. https://doi.org/10.1016/j.ijfatigue.2020.105974
Li K, Yang Z, Zhang Y, Li Y, Lu L, Niu D (2022) Effect of pretreated cow dung fiber on mechanical and shrinkage properties of cementitious composites. J Clean Prod 348:131374. https://doi.org/10.1016/j.jclepro.2022.131374
Ma Y, Wu S, Zhuang J, Tong J, Qi H (2019) Tribological and physio-mechanical characterization of cow dung fibers reinforced friction composites: an effective utilization of cow dung waste. Tribol Int 131:200–211. https://doi.org/10.1016/j.triboint.2018.10.026
Manikandan R, Arjunan TV, Akhil R, Nath OP (2020) Studies on micro structural characteristics, mechanical and tribological behaviours of boron carbide and cow dung ash reinforced aluminium (Al 7075) hybrid metal matrix composite. Compos Part B Eng 183:107668. https://doi.org/10.1016/j.compositesb.2019.107668
Marin-Batista JD, Villamil JA, Qaramaleki SV, Coronella CJ, Rubia M (2020) Energy valorization of cow manure by hydrothermal carbonization and anaerobic digestion. Renew Energy. https://doi.org/10.1016/j.renene.2020.07.003
Masud MH, Ananno AA, Arefin AME, Ahamed R, Das P, Joardder MUH (2019) Perspective of biomass energy conversion in Bangladesh. Clean Technol Environ Policy 21:719–731. https://doi.org/10.1007/s10098-019-01668-2
Min ZR, Zhang MQ, Liu Y, Yang GC, Han MZ (2001) The effect of fiber treatment on the mechanical properties of unidirectional sisal-reinforced epoxy composites. Compos Sci Technol 61:1437–1447. https://doi.org/10.1016/S0266-3538(01)00046-X
Narayan V, Li B, Timmons L (2018) Harnessing the energy potential of cattle dung in India: a policy memorandum to the ministry for new and renewable energy. J Sci Policy Gov 12:1–7. https://doi.org/10.4324/9781936331864-25
Ojedokun AT, Bello OS (2016) Sequestering heavy metals from wastewater using cow dung. Water Resour Ind 13:7–13. https://doi.org/10.1016/j.wri.2016.02.002
Park SW, Kim YR, Schapery RA (1996) A viscoelastic continuum damage model and its application to uniaxial behavior of asphalt concrete. Mech Mater 24:241–255. https://doi.org/10.1016/S0167-6636(96)00042-7
Rahman MT, Mohajerani A, Giustozzi F (2020) Possible use of cigarette butt fiber modified bitumen in stone mastic asphalt. Constr Build Mater 263C:120134. https://doi.org/10.1016/j.conbuildmat.2020.120134
Rath SS, Rao DS, Mishra BK (2016) A novel approach for reduction roasting of iron ore slime using cow dung. Int J Miner Process. https://doi.org/10.1016/j.minpro.2016.11.015
Safaei F, Castorena C (2017) Material nonlinearity in asphalt binder fatigue testing and analysis. Mater Des. https://doi.org/10.1016/j.matdes.2017.08.010
Shan L, Shuang T, He H, Ren N (2016) Internal crack growth of asphalt binders during shear fatigue process. Fuel 189:293–300. https://doi.org/10.1016/j.fuel.2016.10.094
Sheng Y, Zhang B, Yang Y, Li H, Chen Z, Chen H (2019) Laboratory investigation on the use of bamboo fiber in asphalt mixtures for enhanced performance. Arab J Sci Eng 44:4629–4638. https://doi.org/10.1007/s13369-018-3490-x
Su Z, Muhammad Y, Sahibzada M, Li J, Zhang L (2019) Preparation and properties of aminated graphene fiber incorporated modified asphalt. Constr Build Mater 229:116836. https://doi.org/10.1016/j.conbuildmat.2019.116836
Sun Y, Wang W, Chen J (2019) Investigating impacts of warm-mix asphalt technologies and high reclaimed asphalt pavement binder content on rutting and fatigue performance of asphalt binder through MSCR and LAS tests. J Clean Prod 219:879–893. https://doi.org/10.1016/j.jclepro.2019.02.131
Szymajda A, Joka M (2021) Assessment of cow dung pellets as a renewable solid fuel in direct combustion technologies. Energies 14:1192. https://doi.org/10.3390/en14041192
Thangavel A, Gopal E (2017) Experimental study on removal of chromium by using cow dung as low cost adsorbents. Int J Intell Eng Syst 10(3):11–20. https://doi.org/10.22266/ijies2017.0430.02
Wang P, Yong W, Zhao K, Dan C, Wong A (2014) Evolution and locational variation of asphalt binder aging in long-life hot-mix asphalt pavements. Constr Build Mater 68:172–182. https://doi.org/10.1016/j.conbuildmat.2014.05.091
Wang H, Liu X, Panos A, Tom S (2018) Rheological behavior and its chemical interpretation of crumb rubber modified asphalt containing warm-mix additives. Transp Res Rec J Transp Res 2672(28):337–348. https://doi.org/10.13140/RG.2.2.26286.82246
Wang D, Falchetto AC, Alisov A, Schrader J, Riccardi C, Wistuba MP (2019) An alternative experimental method for measuring the low temperature rheological properties of asphalt binder by using 4 mm parallel plates on dynamic shear rheometer. Transp Res Rec J Transp Res 2673(3):427–438. https://doi.org/10.1177/0361198119834912
Wang D, Falchetto AC, Riccardi C, Wistuba MP (2020) Investigation on the low temperature properties of asphalt binder: glass transition temperature and modulus shift factor. Constr Build Mater 245:118351. https://doi.org/10.1016/j.conbuildmat.2020.118351
Xiang Y, Xie Y, Long G (2018) Effect of basalt fiber surface silane coupling agent coating on fiber-reinforced asphalt: From macro-mechanical performance to micro-interfacial mechanism. Constr Build Mater 179:107–116. https://doi.org/10.1016/j.conbuildmat.2018.05.192
Xing X, Liu T, Pei J, Huang J, Tian Y (2020) Effect of fiber length and surface treatment on the performance of fiber-modified binder. Constr Build Mater. https://doi.org/10.1016/j.conbuildmat.2020.118702
Yga B, Yz C, Elo C, Am A, Hs A (2021) Influence of anti-ageing compounds on rheological properties of bitumen. J Clean Prod 318:128559. https://doi.org/10.1016/j.jclepro.2021.128559
Zhang Y, Gao Y (2019) Predicting crack growth in viscoelastic bitumen under a rotational shear fatigue load. Road Mater Pavement Des 22(3):603–622. https://doi.org/10.1080/14680629.2019.1635516

Zhou F, Mogawer W, Li H, Andriescu A, Copeland A (2013) Evaluation of fatigue tests for characterizing asphalt binders. J Mater Civ Eng 25:610–617. https://doi.org/10.1061/(asce)mt.1943-5533.0000625